Fluorescent polysome profiling reveals stress-mediated regulation of HSPA14-ribosome interactions

Anatoly Meller[1], David Coombs[2], Reut Shalgi[1,*]

[1] Department of Biochemistry, Rappaport Faculty of Medicine, Technion–Israel Institute of Technology, Haifa 31096, Israel

[2] BioComp Instruments, Canada

*To whom correspondence should be addressed: reutshalgi@technion.ac.il

Abstract

Ribosome-associated factors play important roles in regulation of translation in response to various physiological and environmental signals. Here we present fluorescent polysome profiling, a new method that provides simultaneous detection of UV and fluorescence directly from polysome gradients. We demonstrate the capabilities of the method by following the polysome incorporation of different fluorescently tagged ribosomal proteins in human cells. Additionally, we used fluorescent polysome profiling to examine chaperone-ribosome interactions, and characterized their changes in response to proteotoxic stresses. We revealed dynamic regulation of HSPA14-polysome association in response to heat shock, showing a marked heat shock-mediated increased in the polysome-association of HSPA14. Our data further support a model whereby HSPA14 dimerization is increased upon heat shock. We therefore established fluorescent polysome profiling as a powerful, streamlined method that can significantly enhance the study of ribosome-associated factors and their regulation.

Introduction

Regulation of protein translation, allowing fast changes in protein levels, is necessary for a timely cellular response to changing environmental or internal conditions [1]. Translation regulation can occur globally, through control of various translation factors involved in the different stages of translation. i.e. initiation, elongation or release factors [2,3]. Translation can also be controlled specifically, at the level of single or groups of mRNAs, or at the level of nascent chains, often through ribosome associated factors [4,5]. The ribosome itself is also increasingly being implicated in regulation of translation, with specialized ribosomes interacting differentially with specific subsets of mRNAs [6,7].

A commonly used method for assessing global translation levels and changes is polysome profiling, which involves separation of polyribosome complexes by density using sucrose gradients centrifugation and measuring the optical density along the gradient. The resulting curve allows to measure the amounts of RNA bound by mono- and poly-ribosomes, which is used as a proxy for the overall translation levels in the cell.

A large variety of ribosome-interacting proteins have been demonstrated to affect translation either globally, or for specific mRNAs [5,8]. Examples include the microRNA machinery, various RNA binding proteins, and more [5,8]. Therefore, the specific functions and the dynamic interactions of ribosome-associated factors are of great interest.

Molecular chaperones have long been known to interact with ribosomes, and aid in the holding of nascent chains and folding of newly synthesized proteins [4,9]. More recently, accumulating evidences suggest that chaperones, being the sensors of the protein homeostasis state in the cells, can play an active role in regulation of translation in response to perturbations in proteostasis [10-13]. Indeed, we and others have previously shown that HSP70-ribosome association is reduced in response to proteotoxic stress in mouse and human cells [10,11]. The ribosome association of the NAC chaperone (Nascent chain Associated Complex) has been shown to be reduced in response to protein aggregation

conditions in nematodes [12]. Therefore, the dynamics and regulation of ribosome-associated factors, including chaperones, is of growing interest.

Nevertheless, the dynamics of the ribosome association of different proteins is often difficult to follow. The most widely used method to assay the ribosome-association of proteins has been fractionation of polysome profiles, followed by protein extraction from the different gradient fractions, and subsequent western blotting. This method is laborious, especially when looking to compare different conditions, depends on accurate fractionation across different gradients, and thus less reproducible. More recently, fluorescence monitoring of polysome fractions was performed after fractionation, using fluorescently tagged ribosomal proteins in *E.coli*, to examine ribosome assembly intermediates [14], improving the efficiency of the traditional method.

Here we present a new technology called fluorescent polysome profiling, which is an easy and streamlined method for interrogation of polysome-associated factors. This method uses a new flowcell instrument that provides an integrated, simultaneous measurement of UV (260nm, for RNA absorbance) and fluorescence, which is combined with a polysome gradient station. We used the instrument to measure UV and fluorescence from polysome profiles of lysates from human HEK293T cells expressing a variety of GFP-tagged proteins, in order to monitor their continuous co-migration with polysomes. This allowed us to obtain high resolution measurements of polysome-association for different proteins, first ribosomal proteins (RPs) and then chaperones, and examine their dynamic association in response to proteotoxic stress conditions.

Results and Discussion

Fluorescent polysome profiling – a new method for detection and quantification of polysome-associated proteins

Fluorescent polysome profiling is a new method for detection and quantification of the polysomal distribution of ribosome components, or the assay of polysome-association of any ribosome associated factor of interest, simultaneously with the generation of the

traditional UV-based polysome profiles. The method relies on the Triax™ flowcell, an instrument that provides an integrated, simultaneous measurement of UV (260nm, for RNA absorbance) and fluorescence directly from gradients.

In order to determine that the flowcell is able to reliably detect ribosome-associated fluorescent proteins, we tested its capabilities using fluorescently-tagged RPs. We first cloned a GFP tag to the ribosomal protein RPLP0 (see Methods), and transfected it into human HEK293T cells. GFP-tagged RPLP0 showed a diffused fluorescence pattern in the cytosol (Fig. 1A). Two days after transfection, we performed fluorescent polysome profiling, and examined the fluorescence signal obtained from the polysome gradients, simultaneously with the UV profile, which provides the levels of RNA at each point in the gradient. We note that the ectopic expression of GFP tagged RPLP0 did not affect the level of translation, as judged by completely overlapping polysome profiles of GFP-only and GFP-tagged RPLP0-transfected cells (Fig. S1A). In parallel, we ran fluorescent polysome profiles of non-transfected cells, and of lysis buffer only. Both polysome profiles of GFP-expressing and GFP-tagged RPLP0-expressing cell lysates were very similar to the profile of non-transfected cells, indicating that translation was overall not affected by the transfection procedure, and by the ectopic expression of fluorescently tagged proteins (Fig. S1B). Both the standard polysome lysis buffer (see Methods) and non-transfected cell lysates gave a low fluorescence background along the gradient (Fig. S1C). Therefore, in all subsequent experiments, a non-transfected cell lysate sample was run in parallel to all GFP-tagged protein samples, and the background fluorescence profile of non-transfected lysates was subtracted from the fluorescence profiles of each GFP-tagged protein that was tested (as illustrated in Fig. S1C,D, see Methods).

As shown in Fig. 1B, while GFP alone concentrated at the top of the gradient (in the unbound fraction), indicating it did not bind ribosomes, RPLP0 fluorescence profile traced the polysome profile almost perfectly, with the exception of the small subunit (40S) peak (see Fig. S1E,F for an additional biological replicate). Indeed, as RPLP0 is a large subunit ribosomal protein, we do not expect to see it in the 40S peak. This indicated that the fluorescent polysome profiling method reliably detected ribosome-incorporated proteins.

Fluorescent polysome profiling can be used with different ribosomal proteins

Next, we GFP-tagged additional RPs, and examined their polysome incorporation using fluorescent polysome profiling. We note that all chosen RPs, including RPLP0 used above, are surface accessible (see RPs marked on the ribosome structure in Fig. S2). The different RPs were expressed at different levels (see Methods, Fig. 1A, S1J). RPS2, a small subunit ribosomal protein, gave a strong fluorescence peak at the 40S subunit, as well as at the 80S monosome peak, and significant fluorescent peaks at the various polysomal fractions (Fig. 1C). Importantly, RPS2 has a negligible peak at the large ribosome subunit area of the gradient (Fig. 1C, see Fig. S1G for an additional biological replicate). This further confirms the specificity of fluorescent polysome profiling.

GFP-tagged RPL28 was relatively lowly expressed (Fig. S1J), yet the instrument was still able to detect its ribosomal incorporation, demonstrating the sensitivity of the method. The fluorescence profile of GFP-tagged RPL28 largely followed that of the polysome profile, with the exception of the 40S peak, again, as expected from a large subunit RP (Fig. 1D, see Fig. S1H for an additional biological replicate). Finally, RPL10A, which has been previously used for ribosome pulldown assays [15], showed a strong fluorescence profile (Fig. 1E, Fig. S1I). RPL10A profiles also showed several strong peaks at the pre-80S region of the gradient, apart from the expected 60S subunit peak. Using microscopy imaging, we observed, in addition to the diffused cytoplasmic pattern, strong nuclear punctae consistent with nucleoli localization (Fig. 1A). Thus, it is possible that the pre-80S peaks observed in the fluorescent polysome profiles correspond to different stages in the assembly of ribosome subunits. Future studies will determine the nature of these peaks.

Investigating ribosome-associated chaperones regulation using fluorescent polysome profiling

We next decided to use fluorescent polysome profiling to examine the ribosome-association of different chaperones. Chaperones have been known to associate with ribosomes, and with newly synthesized nascent chains [9]. We focused on the two chaperone

systems known to interact with ribosomes, namely the Nascent polypeptide-Associated Complex (NAC) and the Hsp70-mRAC system [4,16,17]. The NAC chaperone is a heterodimer, composed of NACA and BTF3, that associates with the ribosome and interacts with nascent polypeptides as they emerge from the ribosome exit tunnel [17]. The mammalian Ribosome Associated Complex (mRAC) co-chaperone system is a ribosome-specific co-chaperone system for the cytosolic Hsp70[18-20], while it is recruited to ribosomes and interacts with nascent chains [21-23]. The mRAC system is comprised of the HSP40 family member MPP11, also known as DNAJC2, a co-chaperone that is essential for the stimulation of the ATPase activity and chaperone action of Hsp70, and the HSP70 like protein HSPA14, also known as HSP70L1 [18-20]. mRAC associates with the ribosome via MPP11 [24,25], and together with Hsp70 interacts with the nascent polypeptide.

We therefore performed fluorescent polysome profiling on cells transfected with either GFP-tagged human BTF3, the beta subunit of the NAC chaperone, or human HSPA14, a subunit of mRAC. Furthermore, as many chaperones, including Hsp70, are known to play a central roles in the regulation of protein homeostasis in response to proteotoxic stresses [26], we wanted to examine potential regulation of the polysome-association of each of these chaperones in response to different perturbations. To that end, we performed fluorescent polysome profiling on transfected cells subjected to each of three proteotoxic stress conditions: heat shock, proteasome inhibition, or ER stress (see Methods).

GFP-tagged BTF3 showed a robust polysome-association under normal growth conditions (Fig. 2A, independent biological replicate presented in Fig. S3A). During stress, BTF3 polysome association changed, in a manner that largely followed the global polysome collapse typical for many stress conditions (Fig. 2B-D, independent biological replicate presented in Fig. S3B-D). Thus, the NAC chaperone did not display specific regulation in its ribosome association in the proteotoxic stress conditions examined here.

Fluorescent polysome profiling reveals HSPA14 polysome-association induction following heat shock

Interestingly, examination of the fluorescent polysome profile of GFP-tagged HSPA14 revealed that its ribosome association was markedly increased following heat shock (Fig. 3, independent biological replicate presented in Fig. S3E-H). Previously, we and others showed that Hsp70 ribosome association (specifically, the HSC70 family member) was reduced in heat shock[10] and other proteotoxic stresses[11]. As HSPA14 is a subunit of the mRAC, that serves as co-chaperone for the cytosolic Hsp70s when they associate with the ribosome [9], we initially expected to see ribosomal depletion of HSPA14 during heat stress, similar to that previously shown for Hsp70 [10,11]. Nevertheless, our results showed the opposite trend.

To verify that this result was independent of the position of the GFP tag, we generated, in addition to the C-terminal GFP-tagged HSPA14 shown in Fig. 3, an N-terminal GFP-tagged version of the protein. Here too, we observed the heat shock-mediated induction in the polysome association of HSPA14 (Fig. 4A-B, independent biological replicate presented in Fig. S4A-B). To further validate this finding, and verify that the heat shock-induced polysomal association of HSPA14 was not affected by the relatively large GFP tag, we transfected cells instead with a FLAG-tagged HSPA14, and performed the traditional polysome profiling followed by polysomal fraction collection and western blot (WB). As shown in Fig. 4C (independent biological replicate presented in Fig. S4C), this traditional method similarly demonstrated the marked increase in HSPA14 polysome-association following heat shock, providing further corroboration to the dynamic regulation of HSPA14-polysome association during heat shock.

Hsp70 has been previously shown to form dimers. Dimerization of Hsp70 was observed for both *Homo sapiens* and *E.coli* Hsp70 [27-29], although the functional role of the dimers is still not clear. Since HSPA14 is an Hsp70 homolog, we hypothesized that the observed increase in its association with polysomes might be explained by increased tendency to homo-dimerize in heat shock. In order to test this hypothesis, we performed co-immunoprecipitation (co-IP) experiments of co-transfected FLAG-tagged HSPA14 and GFP-tagged HSPA14, in either untreated cells, or cells subjected to heat shock treatment. Interestingly, we observed a significant increase in HSPA14-HSPA14 interactions

following heat shock (Fig. 4D, independent biological replicate presented in Fig. S5). Importantly, this increase in HSPA14-HSPA14 interaction was unchanged when we pre-treated lysates with RNase (Fig. 4D, S5B, see Methods). This indicated that the observed HSPA14-HSPA14 interactions are independent of RNA, and thus cannot be the result of indirect association through neighboring ribosomes on the same polysome, translating the same mRNA. Therefore, these results suggest a model in which HSPA14 has an increased tendency to form dimers upon heat shock. Future studies will further illuminate the mechanism and regulation of HSPA14 dimer formation, and its effect on stress-mediated translational control.

Conclusions

Together, our experiments established fluorescent polysome profiling as a sensitive, high resolution method for the detection of polysome-association of ribosome-interacting factors. Using this method, we illuminated novel aspects of the dynamics and regulation of ribosome-associated chaperones, in particular, a novel behavior of ribosome-associated HSPA14 in heat stress conditions. Consequently, fluorescent polysome profiling can be used to explore virtually any ribosome-associated factor that can be fluorescently tagged, and reveal new biological insights into the dynamics and regulation of such factors at the ribosome. This easy and streamlined method can potentially be used to replace the traditional, laborious, method thus far used in the field (i.e. polysome fractionation followed by fraction collection to isolate proteins and their detection using WB). Also, it can be used to study a wide variety of proteins for which a reliable antibody is lacking. Furthermore, with the plethora of available resources of cells harboring GFP tagged proteins, from the widely used yeast libraries[30] to GFP-tagged protein mammalian cell lines that are being constantly developed[31,32], and have thus far been extensively used to study protein expression dynamics, localization, and more, the use of fluorescent polysome profiling can become even easier, potentially facilitating and promoting a much broader examination of many additional ribosome-associated factors and their regulation.

Our experiments illustrate the wide range of potential applications of fluorescent polysome profiling. These applications can range from the characterization of ribosome composition, ribosome assembly intermediates, ribosome-associated factors, mRNA-associated factors, and more. Usage of a variant of the flowcell with two different fluorescent sensors will also expand the capabilities of the method, allowing to simultaneously assay two ribosome-associated proteins at the same run.

Fluorescent polysome profiling can also be potentially used to study the polysomal distribution of specific mRNAs, either using fluorescent probes, or through labeling of mRNAs via tethered coat proteins such as the MS2 system [33]. These future applications will require additional calibration steps.

With the growing interest in specialized ribosomes [6,7], which may have important implications on mRNA-specific translation regulation, fluorescent polysome profiling can greatly enhance our understanding of the regulation of ribosome composition in different condition.

Materials and Methods

Cell culture and Transfection

HEK293T cells were grown in standard DMEM supplemented with 10% FBS. For transfection, HEK293T cells ($5*10^6$ cells per plate) were seeded on 10cm plates and transfected using Lipofectamine 2000 reagent on the same day, according to the manufacturer instruction. As GFP alone was much more highly expressed than GFP-tagged proteins, the amount of transfected DNA for the GFP-only plasmid was titrated down such that the fluorescence peak at the unbound fraction matched that of GFP-tagged RPLP0. Twenty-four hours after transfection, cells were split into two 10cm plates. Cells were harvested 48 hours following the original transfection, when they were at approximately 70% cell confluence. Importantly, we made sure to avoid cell crowding as this inhibits overall cellular translation.

Proteotoxic stresses

HEK293T cells transfected with GFP-tagged proteins were subjected to the following proteotoxic stresses: Heat shock: 2 hours at 42°C, ER stress: 2 hours with 1μM Thapsigargin, Proteasome inhibition: 2 hours with 1μM MG132. As a control, 2 hours with 1μl DMSO per 1ml medium was used.

GFP-Tagged proteins

Plasmids expressing GFP-tagged proteins were prepared using the pcDNA3.1 backbone plasmid. RPLP0, RPS2, RPL28, RPL10A, and BTF3 proteins were tagged with an N-terminal GFP tag and cloned into pcDNA3.1 using Gibson cloning. HSPA14 protein was tagged with a C-terminal GFP tag, or with a C-terminal FLAG tag using the pcDNA3.1 backbone plasmid, and with a N-terminal GFP tag using a pT-Rex™-DEST30 plasmid, using gateway cloning.

GFP intensity measurement and Fluorescent microscopy

To measure the expression level of GFP-tagged RPs, GFP fluorescence intensity of cells was measured in live cells, after replacing media with PBS, using Tecan Infinity M200PRO reader. Non-transfected cells were used as background.

Fluorescent imaging of HEK293T cells transfected with GFP-tagged ribosomal proteins was performed with the following exposure times for GFP channel: RPL10A - 400ms, RPL28 - 1000ms, RPLP0 - 200ms, RPS2 - 200ms.

Sucrose gradient formation

Sucrose solutions were prepared according to the following recipe: 25mM HEPES pH 6.9, 100mM KCl, 5mM MgCl2, and 10% or 50% sucrose. Protease inhibitors (Roche tablets cat #11836170001), 100μg/ml CHX (cycloheximide), and 1mM DTT (dithiothreitol) were added immediately before use.

Sucrose gradients of 10%-to-50% sucrose were prepared using BioComp gradient master, according to the manufacturer instruction.

Cell harvesting for fluorescent polysome profiling

Lysis buffer was prepared as follows: 25mM HEPES pH 6.9, 1% Triton X-100, 100mM KCl and 5mM MgCl2. Protease inhibitors (Roche tablets, cat #11836170001), 100µg/ml CHX, 1mM DTT, and RNase inhibitors (SUPERase-In, ThermoFisher, AM2694) were added immediately before use. Cells were incubated with 100µg/ml CHX for 3 minutes at 37 °C, then put on ice, washed once with ice cold PBS with 100µg/ml CHX and collected by scraping in ice cold PBS with 100µg/ml CHX. After pelleting at low speed (300g for 7 minutes at 4°C), cells were resuspended in ice cold lysis buffer. Cellular membranes were disrupted by passing through a 25G syringe needle 5 times. Then, the lysates were centrifuged for 10min at 15000 RPM at 4 °C, and the supernatant was transferred to new tubes. OD units (260nm) were measured using NanoDrop 2000C spectrophotometer.

Fluorescent Polysome Profiling

Sample volumes containing equal number of 260nm OD units (corresponding to the amount of RNA per sample) were loaded onto the sucrose gradients, and centrifuged using an ultracentrifuge for 2 hours at 35,000 RPM at 4°C. UV and GFP polysome profiles were obtained using the Triax™ flowcell (BioComp Instruments). Triax™ flowcell software version 1.45A was used with the following parameters:

Parameter	**Value**
Scanning mode	UV OD WITH SINGLE FLUORESCENCE SCAN
Channel A (LED1) Wavelength	260 nm
Channel B (LED2) Fluor	EGFP
Excitation (LED2) Wavelength	470 nm
Excitation filter A	470/40 nm
Emission filter A	525/50 nm
Sensitivity	0
Integration time	350 ms
LED1 (260 nm) On Time	18 ms
PD2 (470 nm) On Time	350 ms

Equal amount of 260 nm OD units of non-transfected HEK293T cell lysate were ran together with every set of experimental samples. This negative control GFP fluorescence profile was used as background, which was subtracted from every other GFP fluorescence profile in the set of experimental samples.

All fluorescent polysome profile figures were prepared using MATLAB scripts.
For display purposes polysome curves were smoothed using a median filter, with a window of 10 for UV curves and a window of 15 for GFP curves.

Polysomal fractionation followed by WB

Cells transfected with HSPA14-FLAG, either untreated or subjected to HS, were harvested and polysome profiling was performed as above. In parallel, polysomal fractions were collected using a Gilson FC203B fraction collector, with 24 equal volume (450µl) fractions per condition. Following polysome fractionation, the fractions were combined into five pools, the Unbound fraction (fractions 1-3), ribosome Subunits (Sub, 4-6), Monosome (Mono, 7-8), Medium polysomes (Med, 9-14) and Heavy polysomes (Heavy, 15-22). The Sub, Mono, Med and Heavy pools were each diluted to a final volume of 12.5ml with a dilution buffer (20mM HEPES pH 6.9, 0.5% NP-40, 0.5% Sodium Deoxycholate, 100mM KCl and 5mM MgCl2. 100µg/ml CHX was added immediately before use). Then, the Sub, Mono, Med and Heavy pools were layered on top of 12.5ml of sucrose cushion solution (25mM HEPES pH 6.9, 100mM KCl and 5mM MgCl2, and 17.5% sucrose. 100µg/ml CHX was added immediately before use) and centrifuged for 17 hours at 44,000RPM in a type 70 Ti rotor, at 4°C (an equivalent of 100,000G for 24 hours, as in [34]). Subsequently, the remaining ribosome pellets were resuspended in 40ul of protein sample buffer. The Unbound pool was diluted 1:1 with the protein sample buffer, and all samples were boiled at 100°C for 5 minutes. Finally, equal volumes of each fraction pool, corresponding to 0.5% of the Unbound fraction and 37.5% of each of the other fractions, were loaded on a 10% SDS-PAGE gel and immunoblotted with anti-FLAG (Sigma-Aldrich, F1804) and anti-RPL10A (Abcam, ab174318) antibodies.

Co-immunoprecipitation

Co-immunoprecipitation (co-IP) buffer was prepared as follows: 50mM HEPES pH 7.9, 0.5% Triton X-100, 5% glycerol, 150mM NaCl and 5mM MgCl2. Protease inhibitors (Roche tablets, cat# 11836170001), 100µg/ml CHX, 1mM DTT and RNase inhibitors (SUPERase-In, ThermoFisher, AM2694) were added immediately before use. Wash buffer was prepared as follows: 50mM HEPES pH 7.9, 1% Triton X-100, 5% glycerol, 150mM NaCl and 5mM MgCl2. Cells were harvested as for the fluorescent polysome profiling preparation described above, using co-IP buffer for lysis. For RNAse treatment, 1µl RNase If (NEB, M0243) per one 260 nm OD unit was added, and samples were rotated for 55 min at room temperature. Afterwards, 2µl of SUPERase-In (ThermoFisher, AM2694) RNase inhibitor were added to all samples (both treated and untreated with RNase If). Samples were immunoprecipitated using 20µl of EZview Red ANTI-FLAG M2 Affinity Gel beads (Sigma-Aldrich, F2426), which were added to a sample volume containing equal number of 260 nm OD units. Additional co-IP buffer was added to reach a final volume of 1ml per sample. Samples with beads were slowly rotated overnight at 4 °C. Beads were then washed 7 times with 1 ml of wash buffer. Following the last wash, the beads were resuspended in equal volumes of wash buffer, protein sample buffer was added, and the samples were boiled at 100 °C for 5 minutes. Equal volumes were then loaded on an 8% NuPAGE gel, and immunoblotted using anti-FLAG (Sigma-Aldrich, F1804) and anti-GFP (MBL, 598) antibodies.

Figure legends

Figure 1: Fluorescent polysome profiling reliably detects GFP-tagged polysome-incorporated ribosomal proteins.

(A) Fluorescence and bright field imaging of GFP-tagged ribosomal proteins, expressed in human HEK293T cells, was performed 2 days after transfection with the following exposure times for the GFP channel: RPLP0: 200 ms, RPS2: 200 ms, RPL28: 1000 ms, RPL10A: 400 ms. (B) Fluorescent polysome profiling confirms the specific detection of polysome-incorporated GFP-tagged RPLP0. Free GFP protein remains in the unbound fraction of the polysome curve (orange curve, left panel), while the fluorescence profile of GFP-tagged RPLP0 lysates (orange curve, right panel) closely follow that of the UV, RNA-

based, polysome profile (blue curve). (C-E) GFP-tagged ribosomal proteins RPS2 (C), RPL28 (D) and RPL10A (E) all show ribosome incorporation using fluorescent polysome profiling.

Figure 2: Fluorescent polysome profiling of NAC chaperone-polysome interactions.
(A) GFP-tagged BTF3 shows a robust polysome association. (B-D) During stress, BTF3 polysome association (orange curve) largely follows the global polysome collapse typical of translation inhibition, as seen by the UV-based profiles (blue curves), which occur after stress. (B) 2h of heat shock (C), proteasome inhibition (using MG132) (D) and ER stress (using Thapsigargin).

Figure 3: HSPA14 polysome association is induced during Heat stress.
(A-D) Examination of a C-terminally GFP-tagged HSPA14 using fluorescent polysome profiling in control and stress conditions (as in Fig. 2). HSPA14 shows a marked increase in polysome association following heat stress (B) compared to control conditions (A).

Figure 4: Induced HSPA14 polysome association in heat stress is accompanied by an increased HSPA14 dimerization.
(A-B) N-terminal GFP-labeled HSPA14 shows a marked increase in polysome interactions following heat stress (B) compared to control conditions (A), similarly to the C-terminal tagged HSPA14 shown in Fig. 3, S3E,F. (C) Polysome profiles of cells transfected with HSPA14-FLAG show an expected heat stress response (top panel). X-axis marks and labels indicate how the fractionated sucrose gradients were pooled for protein extraction (top panel). Western blot of HSPA14-FLAG protein levels (using anti-FLAG antibody) across the polysome gradient in control and heat stressed cells across the different fractions, RPL10A (endogenous) was used as a ribosomal marker (bottom panel). Unbound fraction shows a similar amount of HSPA14-FLAG in both control and heat stress fractions, and contain no detectible RPL10A, as expected. All other fractions show a significant increase of HSPA14-FLAG in heat stress, further corroborating our observation obtained using fluorescent polysome profiling (Fig. 3,4A,B). See Methods for further details. (D) Co-immunoprecipitation revealed an increased HSPA14-HSPA14 interaction following heat stress. HEK293T cells were co-transfected with FLAG-tagged HSPA14 and GFP-tagged

HSPA14 and further subjected to 2h of heat shock. Then immunoprecipitation was performed with anti-FLAG coated beads, and GFP-tagged HSPA14 association was inspected using western blot against GFP. Cells not expressing FLAG-tagged HSPA14 have a minimal GFP background, confirming specificity (lanes 1,2,5,6). After heat shock, HSPA14-HSPA14 interaction is highly increased compared to control cells (lane 4 compared to 3). Additionally, RNase treatment of the samples showed a similar trend (lanes 5-8), indicating that the interaction is not through neighboring ribosomes. See Fig. S5 for input levels and a biological replicate.

Supplementary data

Supplementary Information file contains Supplementary Figures S1-S5.

Acknowledgement

We thank Jeeda Bisharat for her help throughout the project, and Oded Lewinson for helpful discussions. We thank Herman Wolosker, Flonia Levy-Adam and Kinneret Schragenheim-Rozales for critical reading of the manuscript.

Funding

This project has received funding from the European Research Council under the European Union's Horizon 2020 programme Grant 677776.

Authors Contributions

R.S. conceived the study. R.S. and A.M. designed the experiments. D.C. developed the Triax flowcell instrument. A.M. performed all the experiments. R.S. wrote the manuscript with input from A.M.

Conflict of interest

D.C. is the founder and shareholder of BioComp Instruments, a company manufacturing the Triax flowcell.

References

1 Spriggs, K. A., Bushell, M. & Willis, A. E. Translational regulation of gene expression during conditions of cell stress. *Mol Cell* **40**, 228-237, doi:S1097-2765(10)00756-2 [pii] 10.1016/j.molcel.2010.09.028 (2010).

2 Sonenberg, N. & Hinnebusch, A. G. Regulation of translation initiation in eukaryotes: mechanisms and biological targets. *Cell* **136**, 731-745, doi:S0092-8674(09)00090-710.1016/j.cell.2009.01.042 (2009).

3 Dever, T. E. & Green, R. The elongation, termination, and recycling phases of translation in eukaryotes. *Cold Spring Harb Perspect Biol* **4**, a013706, doi:10.1101/cshperspect.a013706 (2012).

4 Preissler, S. & Deuerling, E. Ribosome-associated chaperones as key players in proteostasis. *Trends Biochem Sci* **37**, 274-283, doi:10.1016/j.tibs.2012.03.002 (2012).

5 Harvey, R. F. *et al.* Trans-acting translational regulatory RNA binding proteins. *Wiley Interdiscip Rev RNA* **9**, e1465, doi:10.1002/wrna.1465 (2018).

6 Gilbert, W. V. Functional specialization of ribosomes? *Trends Biochem Sci* **36**, 127-132, doi:10.1016/j.tibs.2010.12.002 (2011).

7 Xue, S. & Barna, M. Specialized ribosomes: a new frontier in gene regulation and organismal biology. *Nat Rev Mol Cell Biol* **13**, 355-369, doi:10.1038/nrm3359 (2012).

8 Simsek, D. *et al.* The Mammalian Ribo-interactome Reveals Ribosome Functional Diversity and Heterogeneity. *Cell* **169**, 1051-1065 e1018, doi:10.1016/j.cell.2017.05.022 (2017).

9 Pechmann, S., Willmund, F. & Frydman, J. The ribosome as a hub for protein quality control. *Molecular cell* **49**, 411-421, doi:10.1016/j.molcel.2013.01.020 (2013).

10 Shalgi, R. *et al.* Widespread regulation of translation by elongation pausing in heat shock. *Molecular cell* **49**, 439-452, doi:10.1016/j.molcel.2012.11.028 (2013).

11 Liu, B., Han, Y. & Qian, S. B. Cotranslational Response to Proteotoxic Stress by Elongation Pausing of Ribosomes. *Molecular cell*, doi:10.1016/j.molcel.2012.12.001 (2013).

12 Kirstein-Miles, J., Scior, A., Deuerling, E. & Morimoto, R. I. The nascent polypeptide-associated complex is a key regulator of proteostasis. *The EMBO journal* **32**, 1451-1468, doi:10.1038/emboj.2013.87 (2013).

13 Brandman, O. *et al.* A ribosome-bound quality control complex triggers degradation of nascent peptides and signals translation stress. *Cell* **151**, 1042-1054, doi:10.1016/j.cell.2012.10.044 (2012).

14 Nikolay, R. *et al.* Validation of a fluorescence-based screening concept to identify ribosome assembly defects in Escherichia coli. *Nucleic Acids Res* **42**, e100, doi:10.1093/nar/gku381 (2014).

15 Heiman, M. *et al.* A translational profiling approach for the molecular characterization of CNS cell types. *Cell* **135**, 738-748, doi:10.1016/j.cell.2008.10.028 (2008).

16 Zhang, Y., Sinning, I. & Rospert, S. Two chaperones locked in an embrace: structure and function of the ribosome-associated complex RAC. *Nat Struct Mol Biol* **24**, 611-619, doi:10.1038/nsmb.3435 (2017).

17 Raue, U., Oellerer, S. & Rospert, S. Association of protein biogenesis factors at the yeast ribosomal tunnel exit is affected by the translational status and nascent polypeptide sequence. *J Biol Chem* **282**, 7809-7816, doi:10.1074/jbc.M611436200 (2007).

18 Hundley, H. A., Walter, W., Bairstow, S. & Craig, E. A. Human Mpp11 J protein: ribosome-tethered molecular chaperones are ubiquitous. *Science* **308**, 1032-1034, doi:1109247 [pii]
10.1126/science.1109247 (2005).

19 Jaiswal, H. *et al.* The chaperone network connected to human ribosome-associated complex. *Mol Cell Biol* **31**, 1160-1173, doi:MCB.00986-10 [pii]
10.1128/MCB.00986-10 (2011).

20 Otto, H. *et al.* The chaperones MPP11 and Hsp70L1 form the mammalian ribosome-associated complex. *Proc Natl Acad Sci U S A* **102**, 10064-10069, doi:0504400102 [pii]
10.1073/pnas.0504400102 (2005).

21 Beckmann, R. P., Mizzen, L. E. & Welch, W. J. Interaction of Hsp 70 with newly synthesized proteins: implications for protein folding and assembly. *Science* **248**, 850-854 (1990).

22 Nelson, R. J., Ziegelhoffer, T., Nicolet, C., Werner-Washburne, M. & Craig, E. A. The translation machinery and 70 kd heat shock protein cooperate in protein synthesis. *Cell* **71**, 97-105, doi:0092-8674(92)90269-I [pii] (1992).

23 Frydman, J., Nimmesgern, E., Ohtsuka, K. & Hartl, F. U. Folding of nascent polypeptide chains in a high molecular mass assembly with molecular chaperones. *Nature* **370**, 111-117, doi:10.1038/370111a0 (1994).

24 Leidig, C. *et al.* Structural characterization of a eukaryotic chaperone--the ribosome-associated complex. *Nat Struct Mol Biol* **20**, 23-28, doi:10.1038/nsmb.2447 (2013).

25 Lee, K., Sharma, R., Shrestha, O. K., Bingman, C. A. & Craig, E. A. Dual interaction of the Hsp70 J-protein cochaperone Zuotin with the 40S and 60S ribosomal subunits. *Nat Struct Mol Biol* **23**, 1003-1010, doi:10.1038/nsmb.3299 (2016).

26 Richter, K., Haslbeck, M. & Buchner, J. The heat shock response: life on the verge of death. *Mol Cell* **40**, 253-266, doi:S1097-2765(10)00782-3 [pii]
10.1016/j.molcel.2010.10.006 (2010).

27 Morgner, N. *et al.* Hsp70 forms antiparallel dimers stabilized by post-translational modifications to position clients for transfer to Hsp90. *Cell Rep* **11**, 759-769, doi:10.1016/j.celrep.2015.03.063 (2015).

28 Thompson, A. D., Bernard, S. M., Skiniotis, G. & Gestwicki, J. E. Visualization and functional analysis of the oligomeric states of Escherichia coli heat shock protein 70 (Hsp70/DnaK). *Cell Stress Chaperones* **17**, 313-327, doi:10.1007/s12192-011-0307-1 (2012).

29 Qi, R. *et al.* Allosteric opening of the polypeptide-binding site when an Hsp70 binds ATP. *Nat Struct Mol Biol* **20**, 900-907, doi:10.1038/nsmb.2583 (2013).

30 Huh, W. K. *et al.* Global analysis of protein localization in budding yeast. *Nature* **425**, 686-691, doi:10.1038/nature02026 (2003).

31 Harikumar, A. *et al.* An Endogenously Tagged Fluorescent Fusion Protein Library in Mouse Embryonic Stem Cells. *Stem Cell Reports* **9**, 1304-1314, doi:10.1016/j.stemcr.2017.08.022 (2017).

32 Sigal, A. *et al.* Dynamic proteomics in individual human cells uncovers widespread cell-cycle dependence of nuclear proteins. *Nat Methods* **3**, 525-531, doi:10.1038/nmeth892 (2006).

33 Bertrand, E. *et al.* Localization of ASH1 mRNA particles in living yeast. *Mol Cell* **2**, 437-445 (1998).

34 Rivera, M. C., Maguire, B. & Lake, J. A. Isolation of ribosomes and polysomes. *Cold Spring Harb Protoc* **2015**, 293-299, doi:10.1101/pdb.prot081331 (2015).

Figure 1

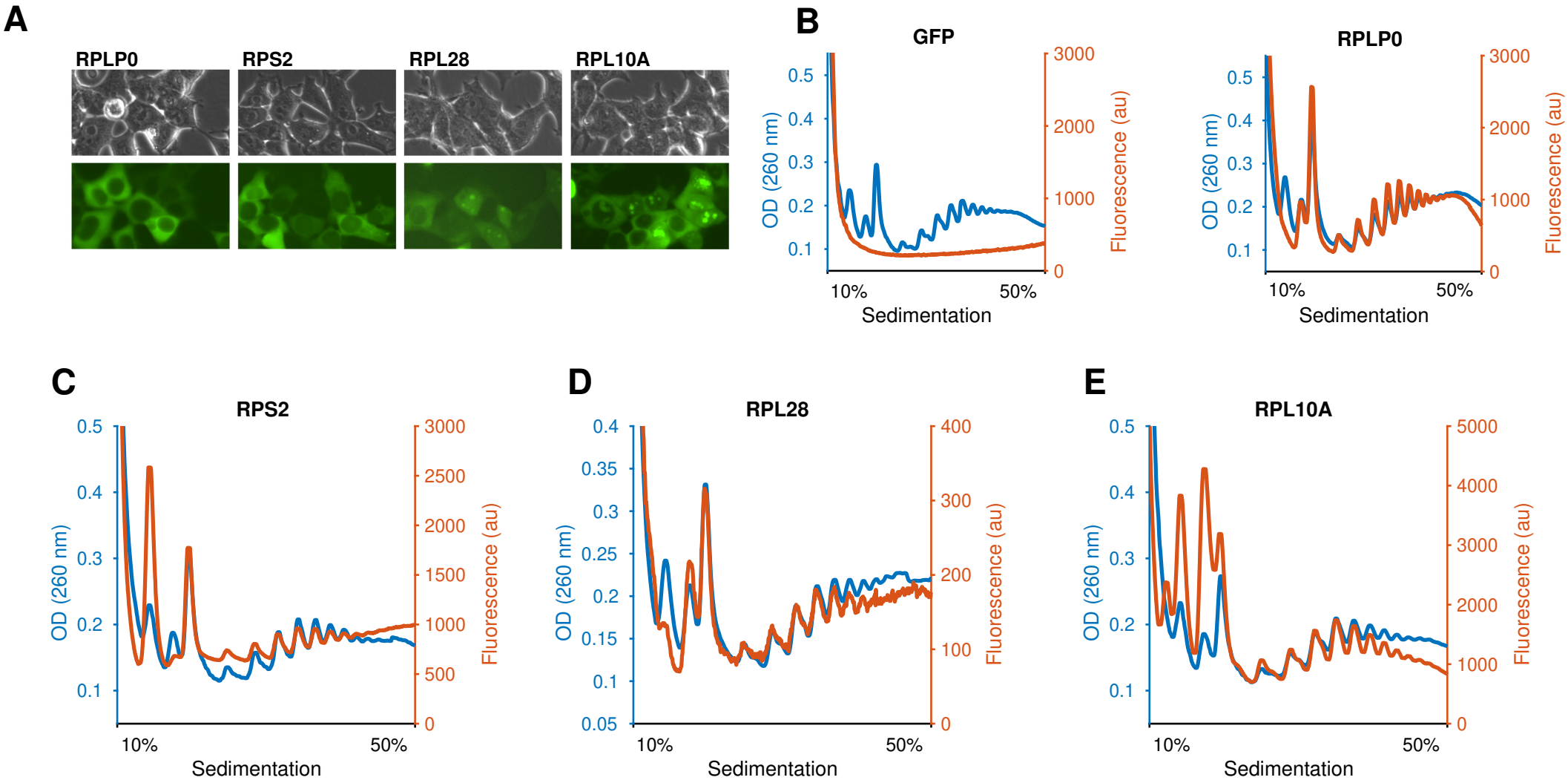
A
RPLP0
RPS2
RPL28
RPL10A
B
GFP
RPLP0
C
RPS2
D
RPL28
E
RPL10A
OD (260 nm)
Fluorescence (au)
10%
50%
Sedimentation

Figure 2

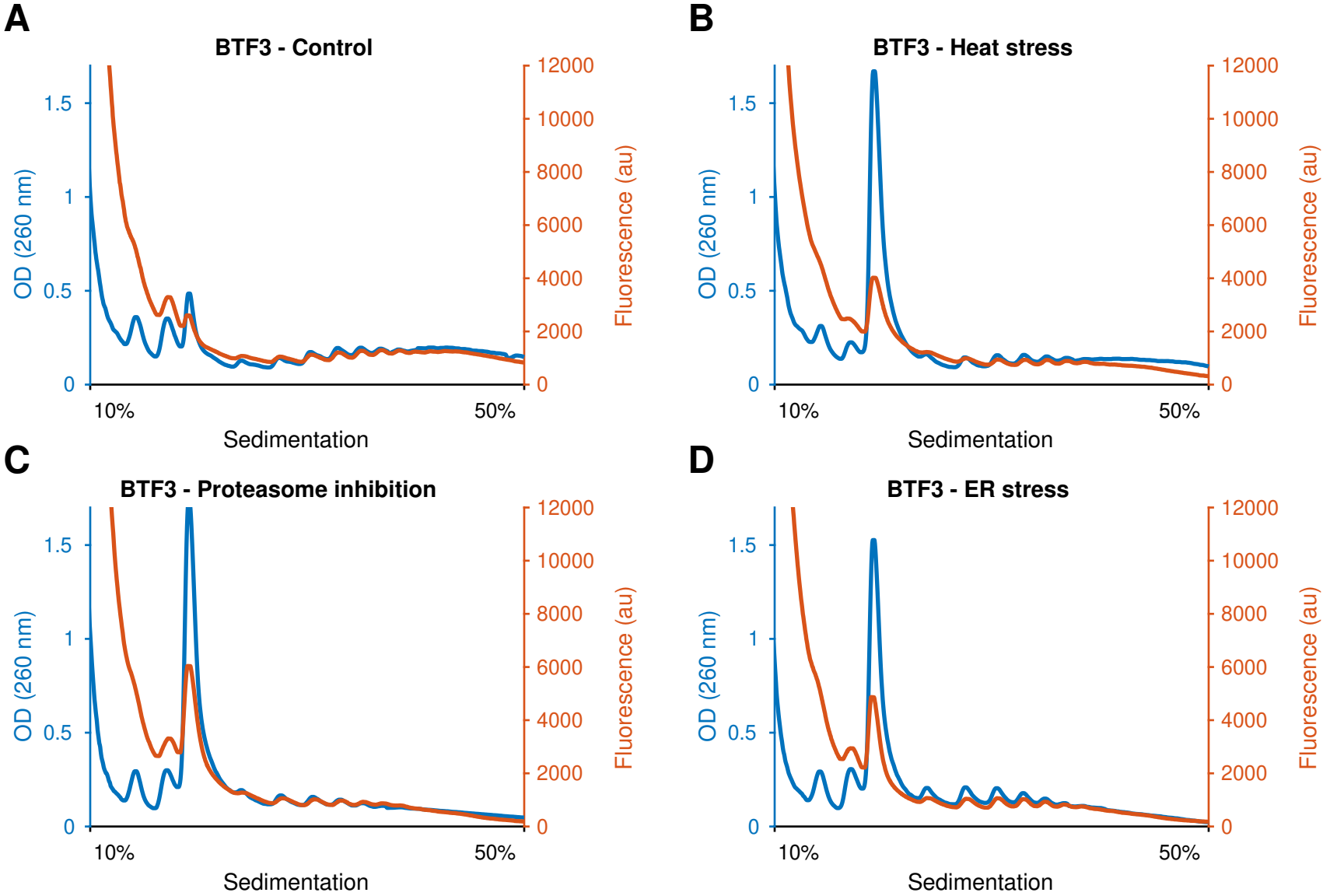
A
BTF3 - Control
B
BTF3 - Heat stress
C
BTF3 - Proteasome inhibition
D
BTF3 - ER stress
OD (260 nm)
Fluorescence (au)
0
0.5
1
1.5
0
2000
4000
6000
8000
10000
12000
10%
50%
Sedimentation

Figure 3

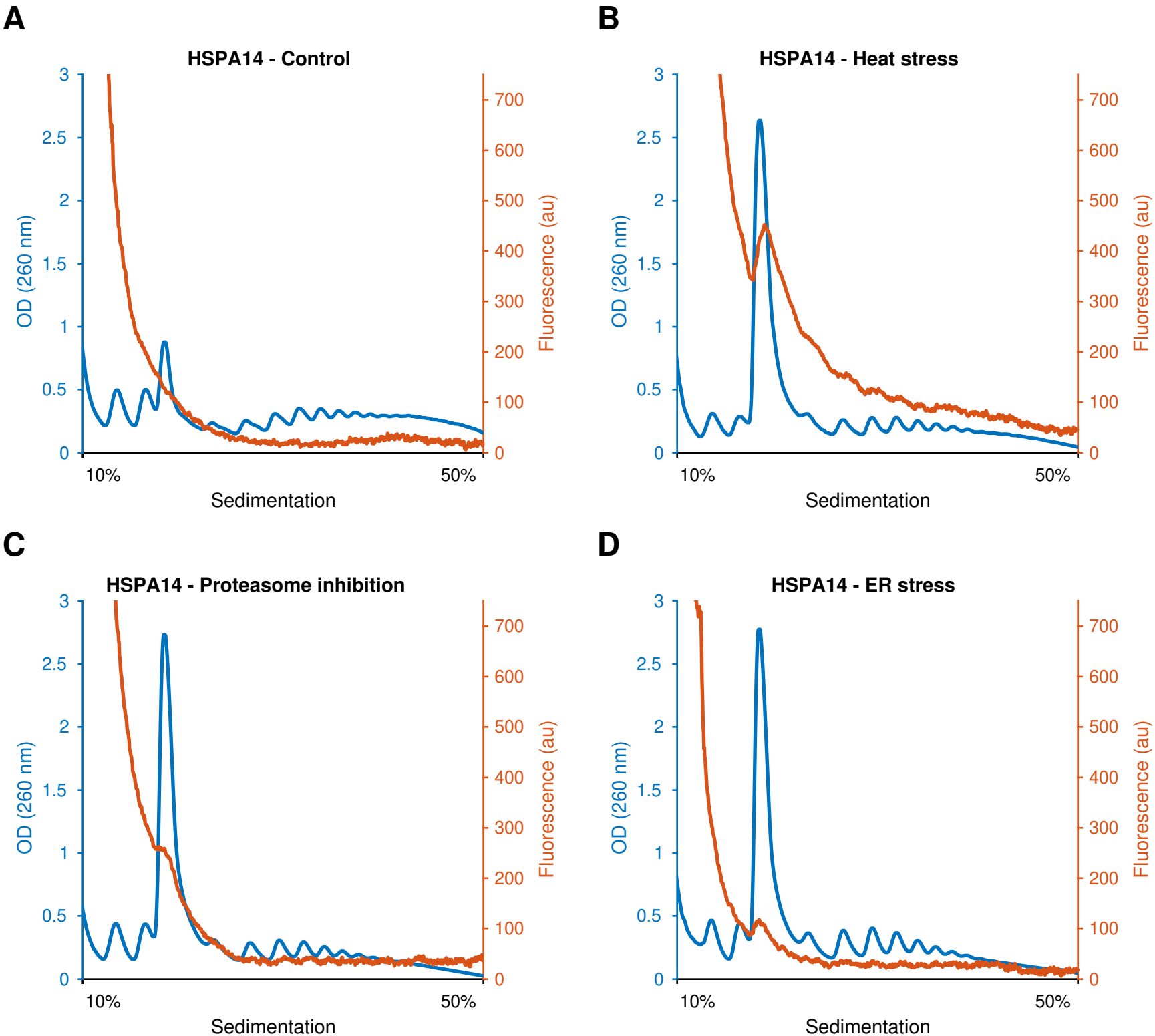
A
HSPA14 - Control
B
HSPA14 - Heat stress
C
HSPA14 - Proteasome inhibition
D
HSPA14 - ER stress
OD (260 nm)
Fluorescence (au)
0
0.5
1
1.5
2
2.5
3
0
100
200
300
400
500
600
700
10%
50%
Sedimentation

Figure 4

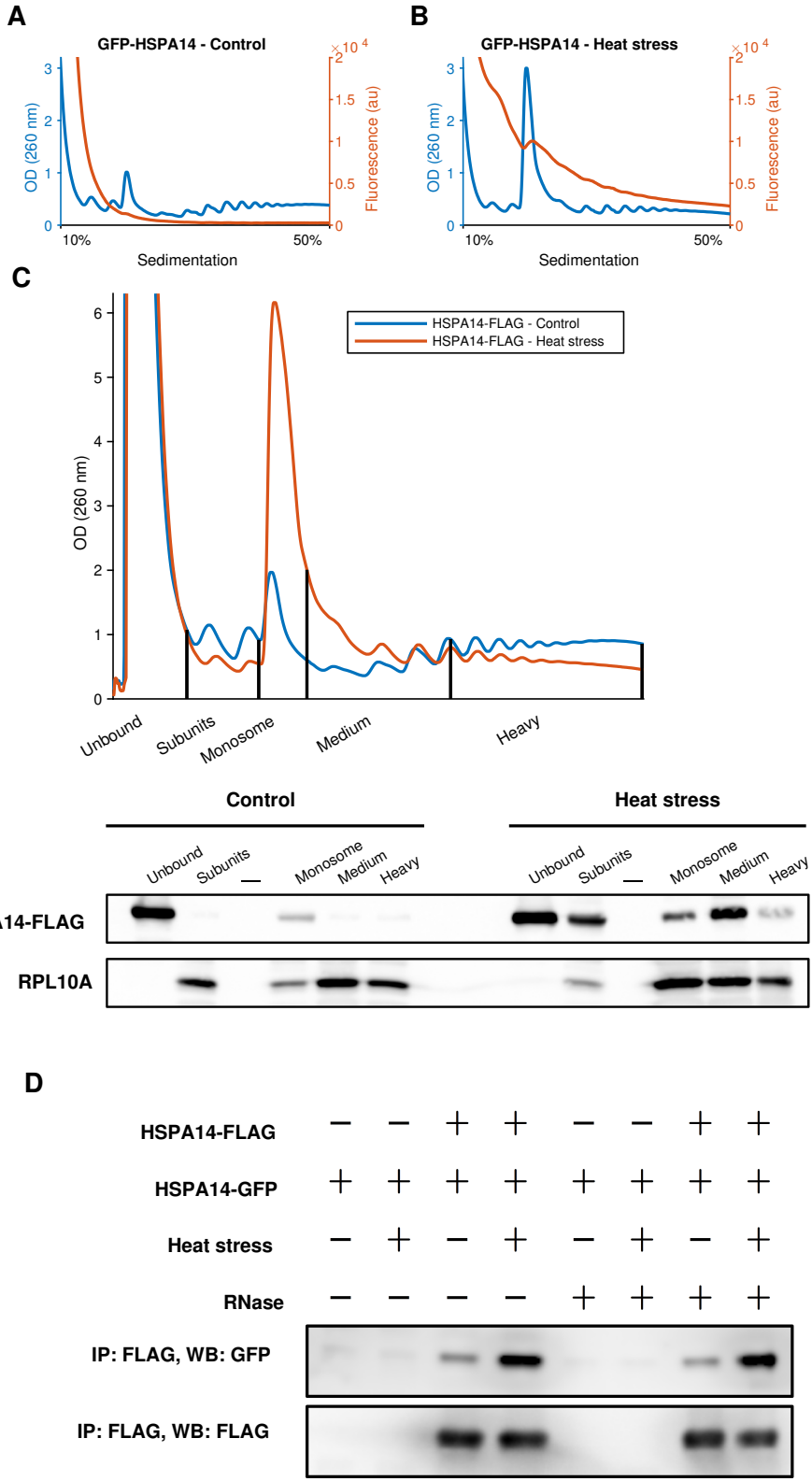
A
GFP-HSPA14 - Control
OD (260 nm)
Fluorescence (au)
×10 4
10%
50%
Sedimentation
B
GFP-HSPA14 - Heat stress
C
HSPA14-FLAG - Control
HSPA14-FLAG - Heat stress
Unbound
Subunits
Monosome
Medium
Heavy
Control
Heat stress
HSPA14-FLAG
RPL10A
D
HSPA14-FLAG
HSPA14-GFP
Heat stress
RNase
IP: FLAG, WB: GFP
IP: FLAG, WB: FLAG